Electronic Supplementary Information

Robust Oil-core Nanocapsules with Hyaluronate-based Shells as Promising NanoVehicles for Lipophilic Compounds

Joanna Szafraniec,[a,b] Agnieszka Błażejczyk,[c] Edyta Kuś,[d] Małgorzata Janik,[a] Gabriela Zając,[a] Joanna Wietrzyk,[c] Stefan Chłopicki*[,d,e] and Szczepan Zapotoczny,*[,a]

[a] Faculty of Chemistry, Jagiellonian University, Gronostajowa 2, 30-387 Krakow, Poland. E-mail: zapotocz@chemia.uj.edu.pl
[b] Department of Pharmaceutical Technology and Biopharmaceutics, Faculty of Pharmacy, Jagiellonian University Medical College, Medyczna 9, 30-688 Krakow, Poland.
[c] Laboratory of Experimental Oncology, Ludwik Hirszfeld Institute of Immunology and Experimental Therapy, Polish Academy of Sciences, Weigla 12, 53-114 Wroclaw, Poland.
[d] Jagiellonian Centre for Experimental Therapeutics (JCET), Jagiellonian University, Bobrzynskiego 14, 30-348 Krakow, Poland. E-mail: stefan.chlopicki@jcet.eu.
[e] Chair of Pharmacology, Jagiellonian University Medical College, Grzegorzecka 16, 31-531 Krakow, Poland.

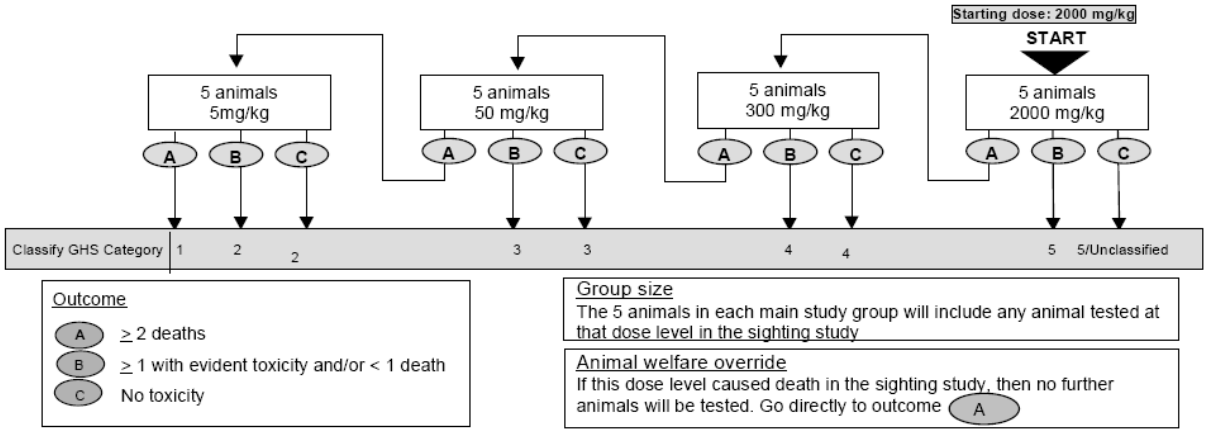

Figure S1 Flow chart of the toxicity main experiment with a starting dose of 2000 mg/kg body weight (according to OECD Guideline 420 – Acute Oral Toxicity – Fixe Dose Procedure).

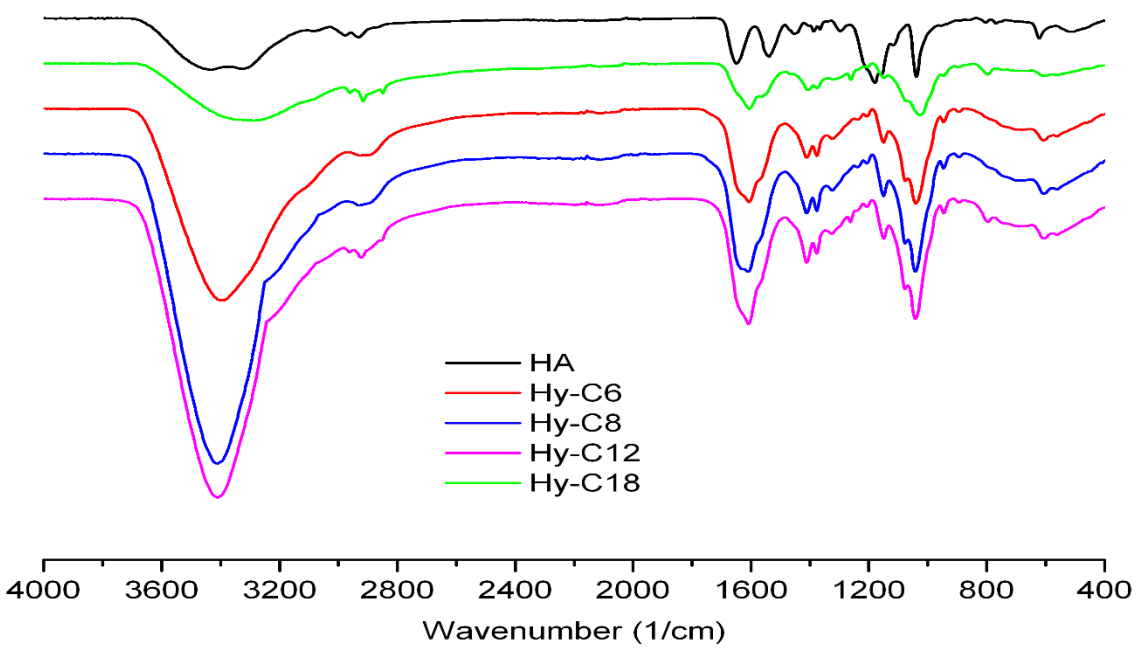

Figure S2 IR spectra of a series of HA derivatives.

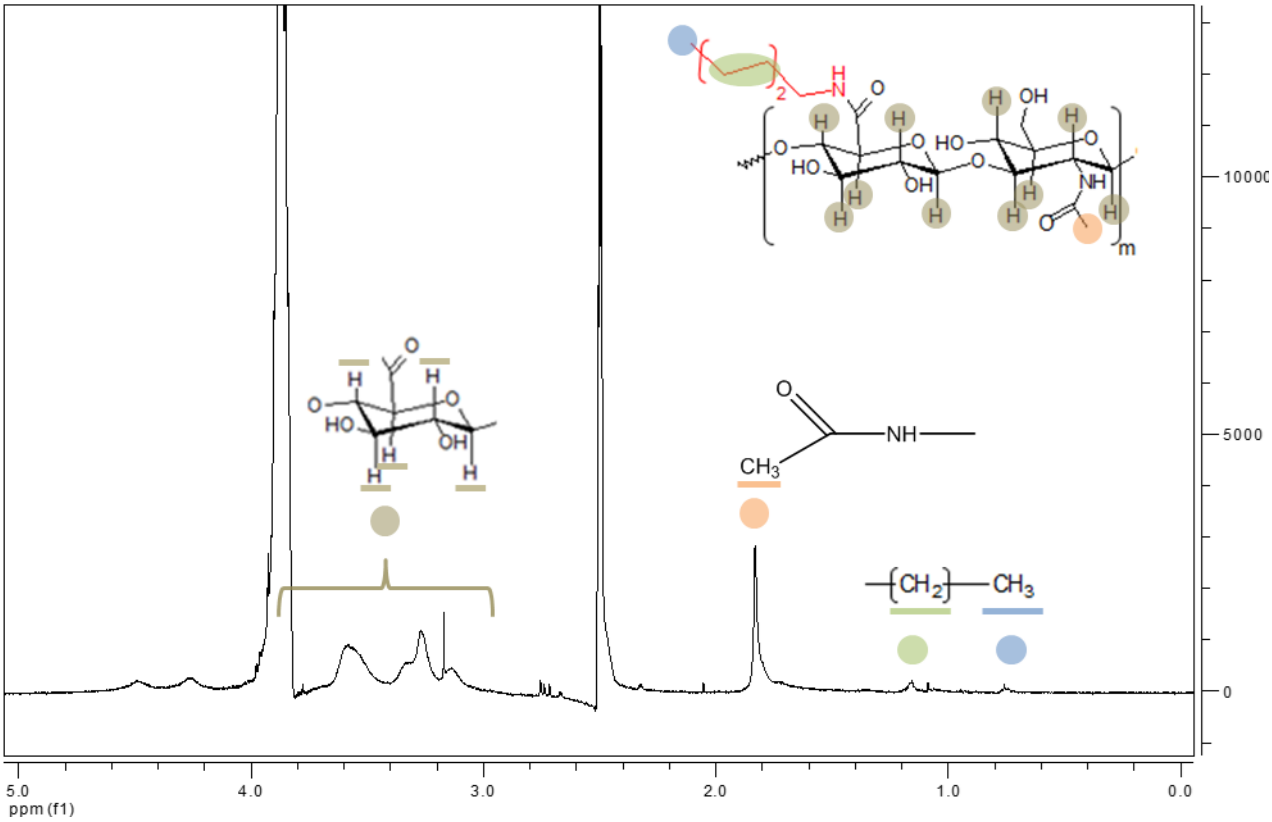

Figure S3 ^{1}H NMR spectrum of Hy-C6 (D2O:DMSO-d6 1:1 v/v).

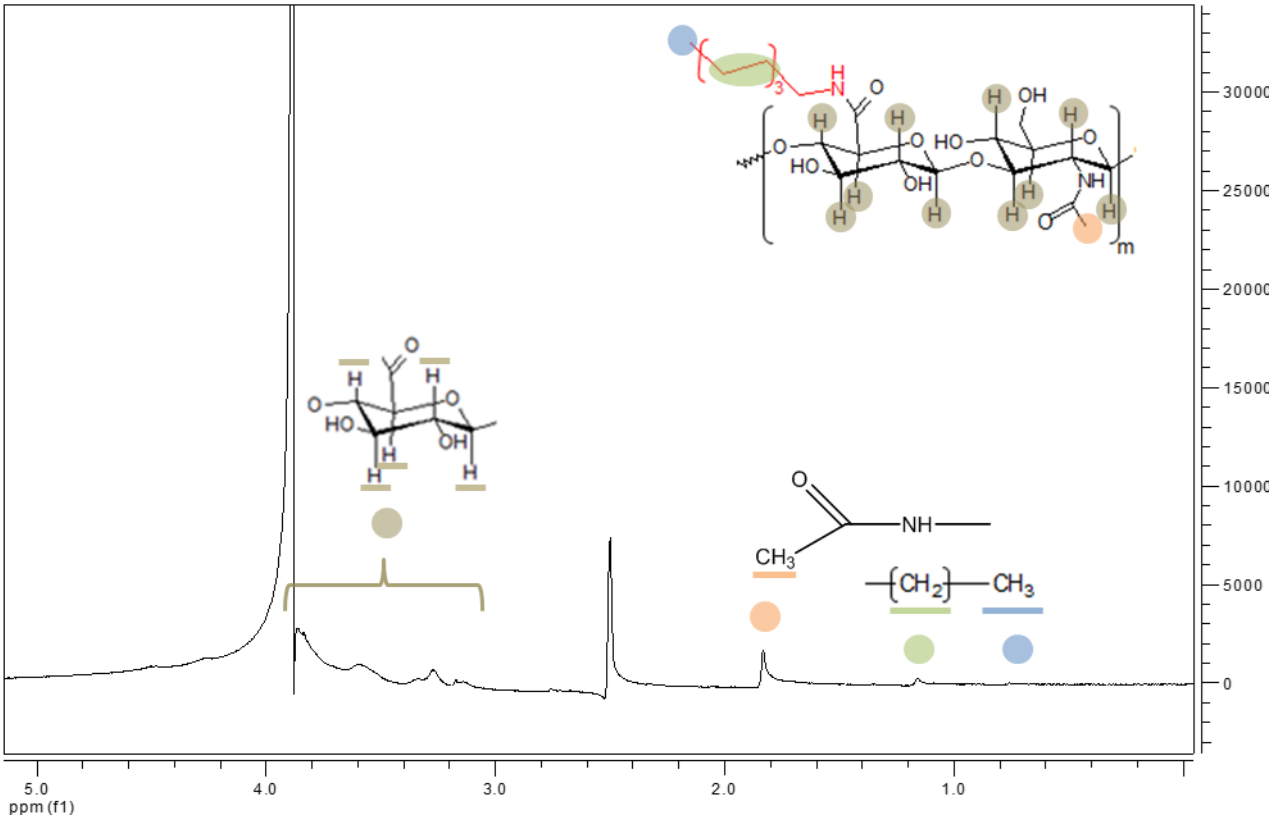

Figure S4 [1]H NMR spectrum of Hy-C8 (D2O:DMSO-d6 1:1 v/v).

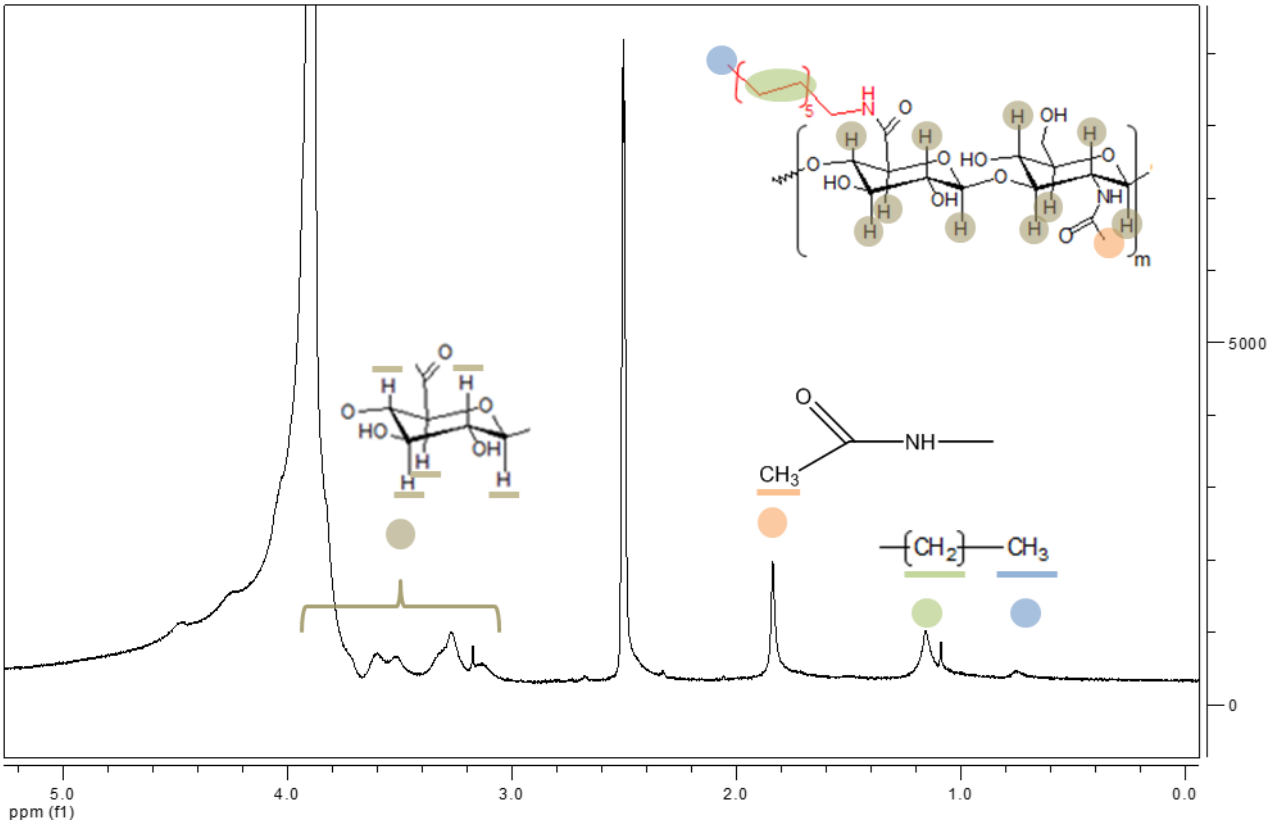

Figure S5 [1]H NMR spectrum of Hy-C12 (D2O:DMSO-d6 1:1 v/v).

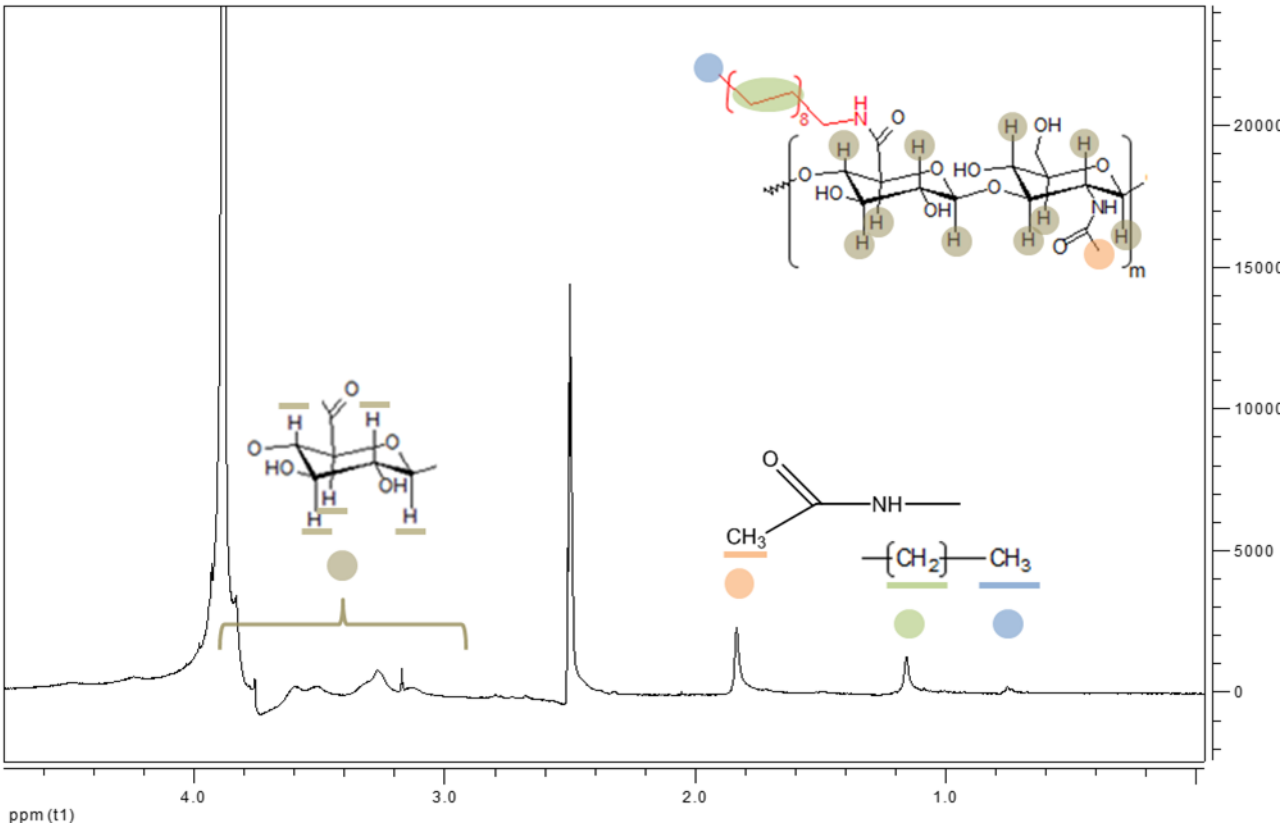

Figure S6 ^{1}H NMR spectrum of Hy-C18 (D2O:DMSO-d6 1:1 v/v).

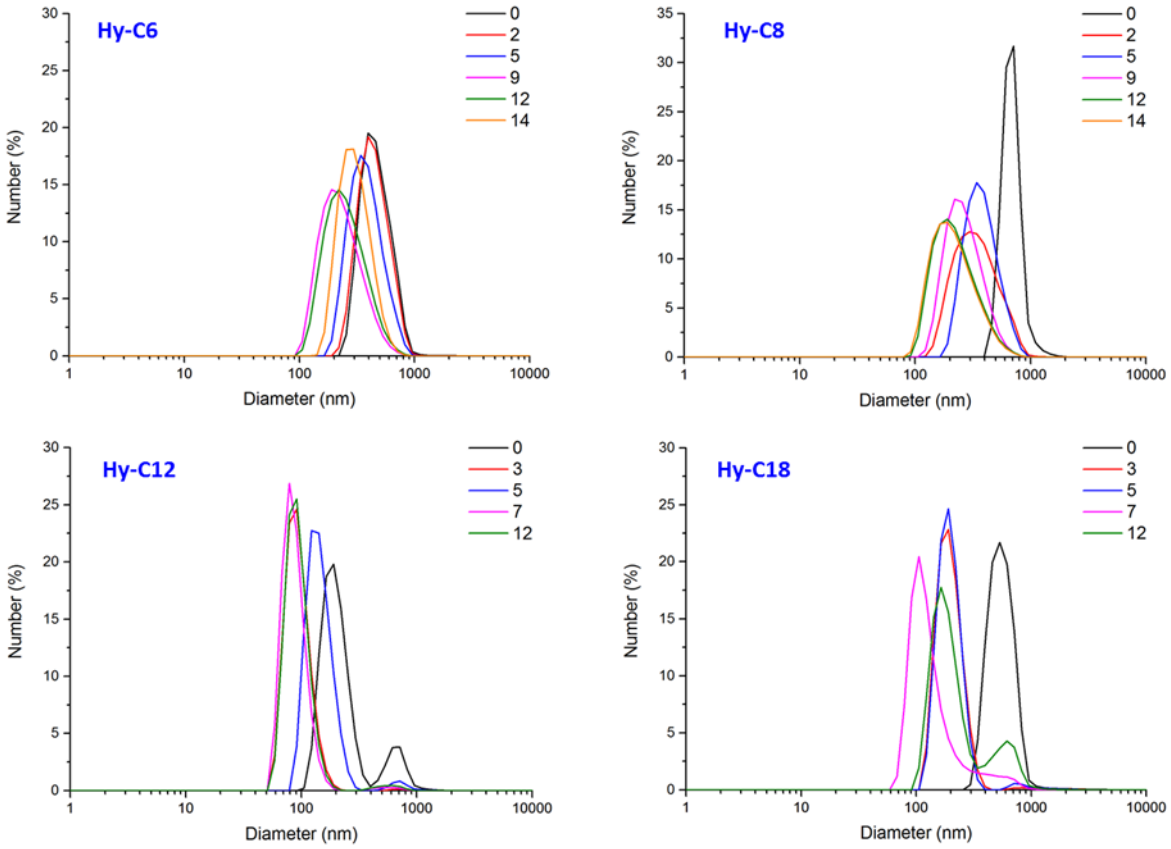

Figure S7 Number-weighted size distribution of capsules stabilized by series of hydrophobically modified hyaluronate.

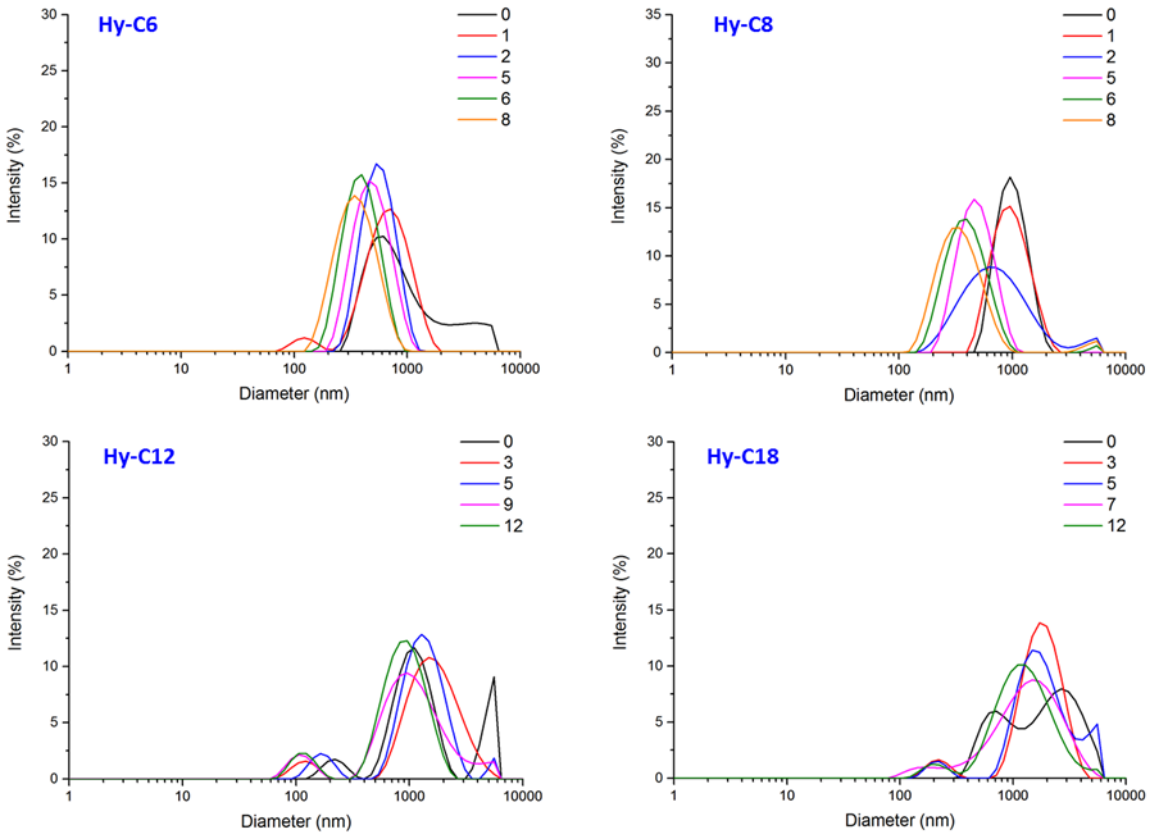

Figure S8 Intensity-weighted size distribution of capsules stabilized by series of hydrophobically modified hyaluronate.

Intensity-weighted particle size distribution indicates formation of typically two fractions of particles, the first one of diameter below 300 nm, and the second one exceeding 600 nm in diameter (Fig. S8). Due to the fact that the intensity of light scattered has a strong dependence on the size of the particles (it is proportional to the sixth power of their diameter) the amount of bigger fraction seems to dominate. However, while comparing results presented in Fig. S7 and S8 one can notice that the number-weighted distribution is wider and mostly monomodal what confirm that small particles are predominant components of the system. Both of the applied methods of averaging of particles' size confirm disintegration of bigger particles as the curves shift towards lower diameters with time.

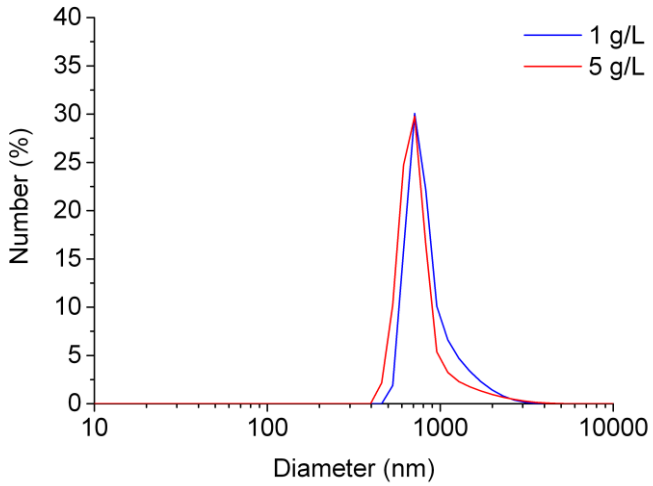

Figure S9 Number-weighted size distribution of capsules Hy-C18x.

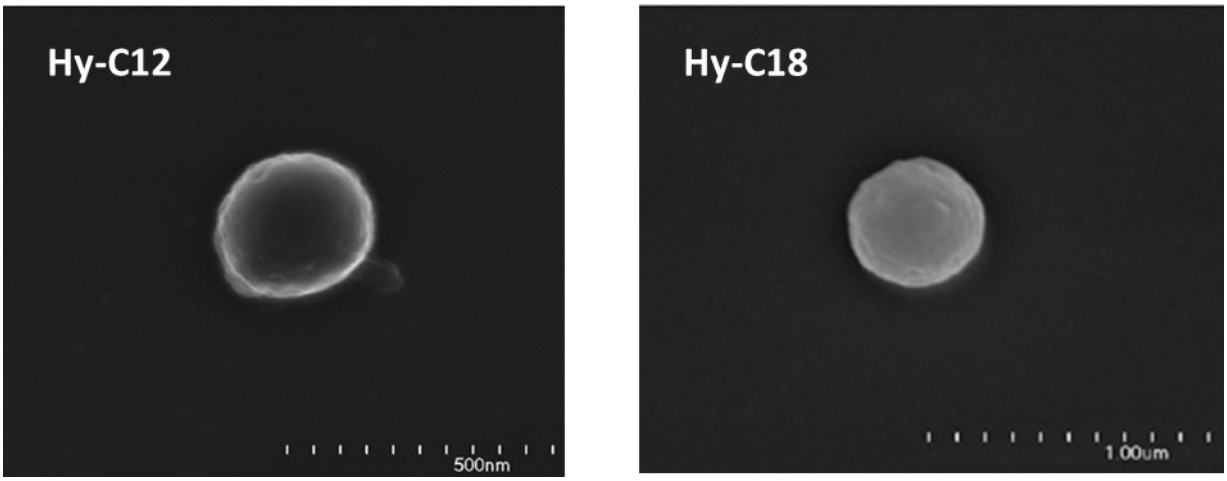

Figure S10 SEM images of capsules stabilized by Hy-C12 and Hy-C18 templated on n-octadecane core.

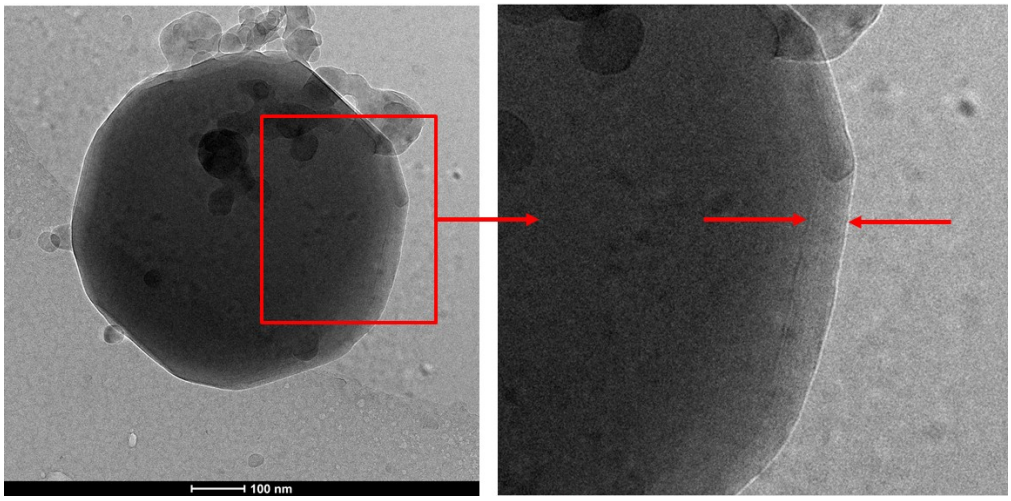

Figure S11 Cryo-TEM image of the capsules stabilized by Hy-C8 templated on oleic acid core.

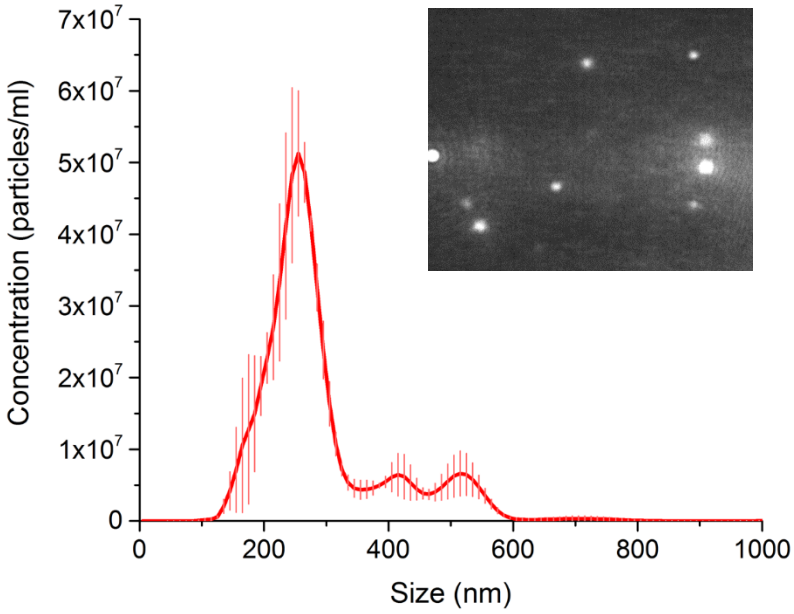

Figure S12 Average particle size distribution profile from NTA measurements for the capsules based on Hy-C12 (red error bars represent ±1 standard deviation of the mean); insert – snapshots from registered nanocapsules dynamics.

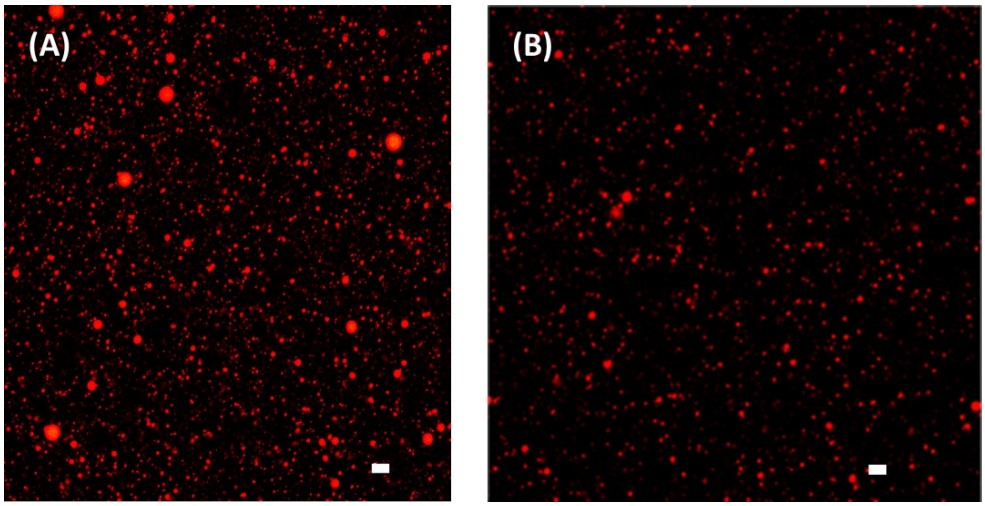

Figure S13 Confocal micrograph of capsules Hy-C12 with encapsulated Nile Red (A) and rhodamine B (B) fluorescent dyes (scale bar 5 μm).

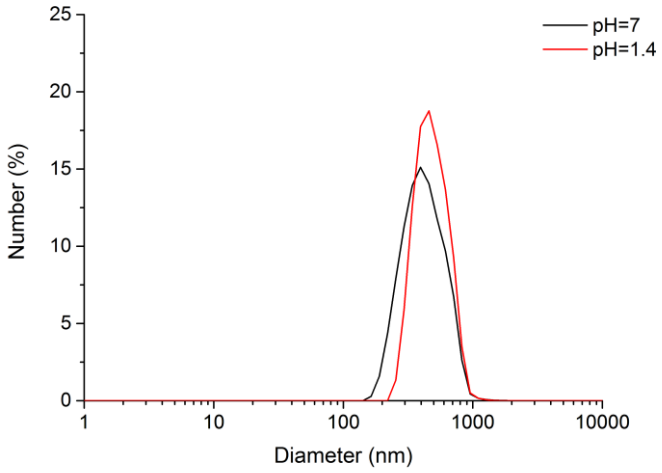

Figure S14 Number-weighted size distribution of Hy-C12 capsules suspended in 0.1M NaCl solution at pH≈7 and pH≈1.4, respectively.

In order to check the applicability of capsules as orally administered delivery system the capsules obtained in 0.1M NaCl solution at pH≈7 were acidified using hydrochloride acid to pH≈1.4. Hydrodynamic diameters of the capsules measured using DLS technique varied only a little, from 280 nm at pH≈7 to 310 nm at pH≈1.4 (Fig. S14). Although the measured apparent zeta potential raised substantially from c.a. -22 mV (at pH≈7) to –1 mV (at pH≈1.4), partially as a result of protonation of carboxylate groups of hyaluronate, the capsules' dispersion remained stable and did not tend to aggregate. It indicates that the obtained nanocapsules are stable in broad pH range enabling also their oral administration (pH of stomach may be as low as 1-2).

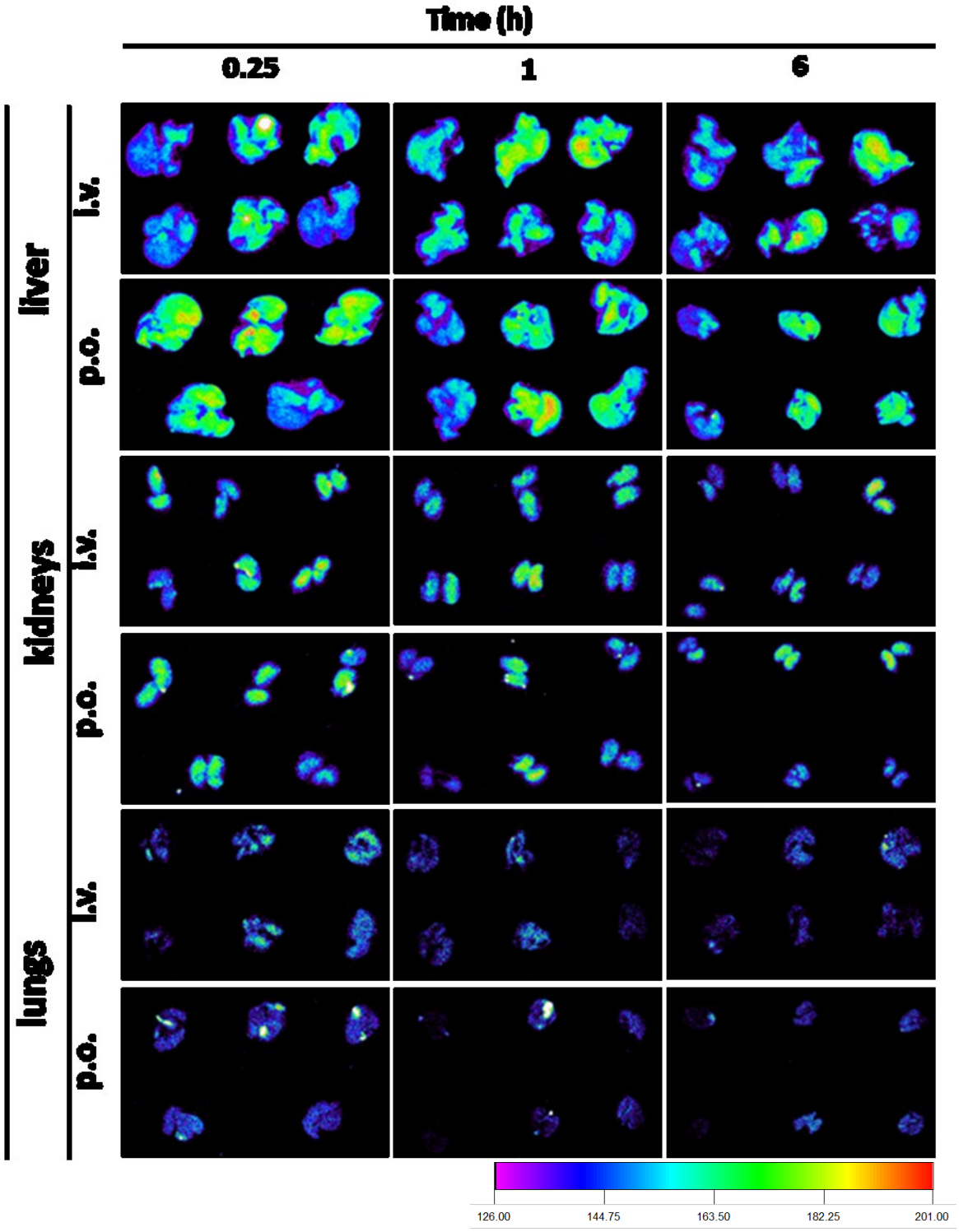

Figure S15 Biodistribution of capsules measured *ex vivo* in organs isolated from mice (organ in right lower panel is from a control mouse) – experiment without LPS.

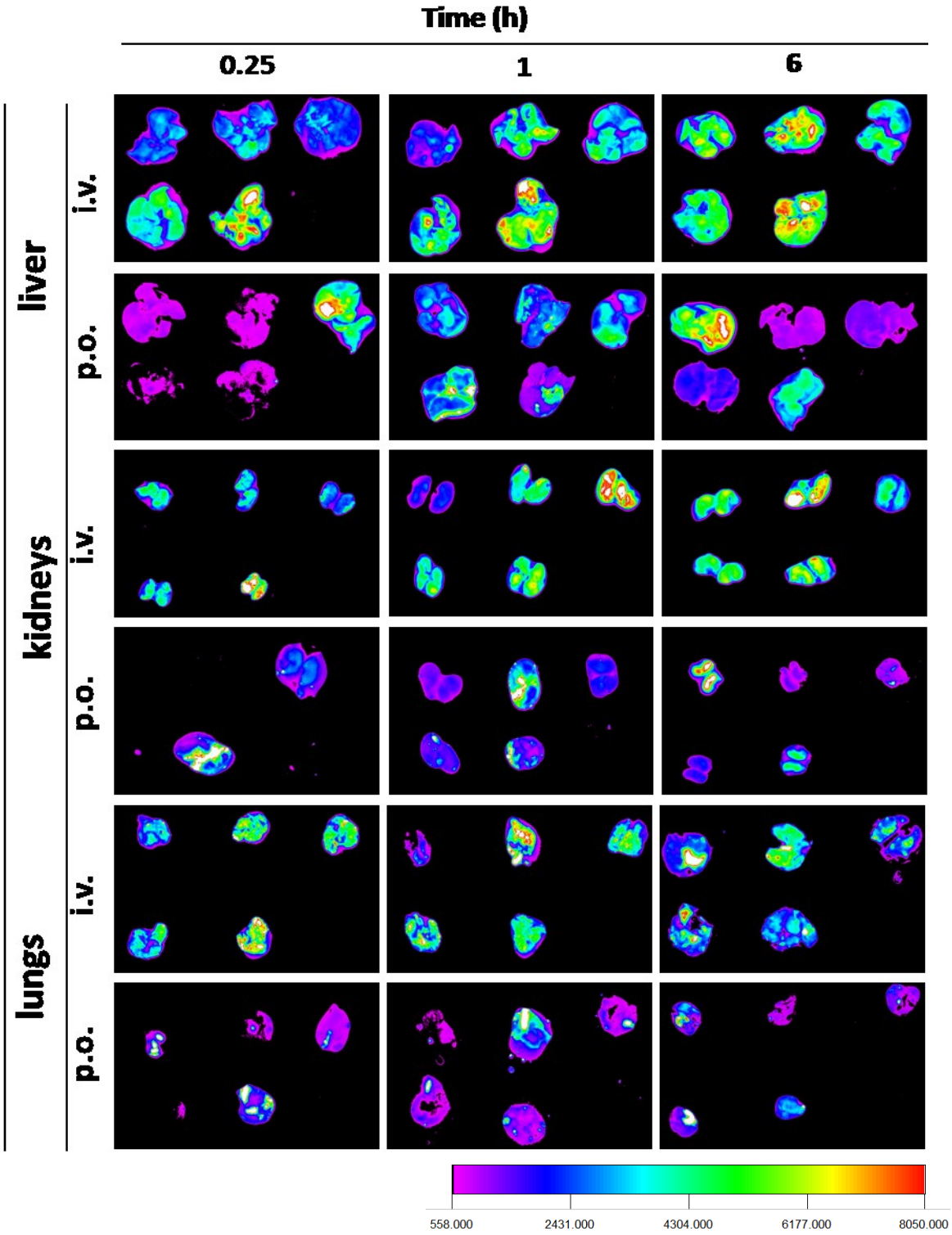

Figure S16 Biodistribution of capsules measured *ex vivo* in organs isolated from mice (organ in right lower panel is from a control mouse) – experiment with LPS.

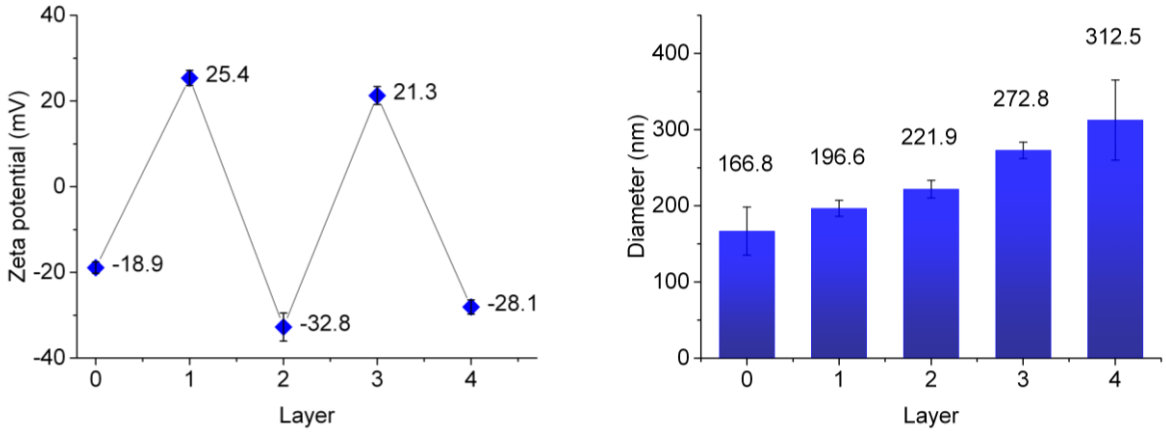

Figure S17 Zeta potential (left) and number-weighted size (right) of capsules Hy-C12 as a function of number of alternating CChit and AChit layers (0-bare capsules).

Table S1 Fluorescence intensity ratios measured *ex vivo* in organs isolated from mice being administered capsules intravenously or orally – LPS experiment.

LPS	**$I_{i.v.}/ I_{p.o.}$**		
t (h) / **Organ**	**0.25**	**1**	**6**
Liver	6.7	3.3	2.1
Kidneys	3.3	1.6	2.6
Lungs	2.8	1.2	3.3